Development of a fiber structure in poly(vinylidene fluoride) by a CO_2 laser heated drawing process

YoungAh Kang[1], KyoungHou Kim[2], Soichiro Ikehata[1], Yutaka Ohkoshi[1*], Yasuo Gotoh[1], Masanobu Nagura[1], Mitsuharu Koide[3], Hiroshi Urakawa[3]

[1] Faculty of Textile Science and Technology, Shinshu University, 3-15-1 Tokida, Ueda, Nagano 386-8567, Japan; fax +81-268-21-5454; yakang@shinshu-u.ac.jp; yokoshi@shinshu-u.ac.jp

[2] Collaborative Innovation Center for Nanotech FIBER (nanoFIC), Shinshu University, Ueda, Nagano 386-8567, Japan; Khkim@shinshu-u.ac.jp

[3] Faculty of Engineering and Design, Kyoto Institute of Technology, Goshokaidoucho, Matsugasaki, Sakyo-ku, Kyoto 606-8585, Japan

ABSTRACT:

Rapid and uniform heating by CO_2 laser radiation can fix the position where necking occurs, so this study investigated the development of a fiber structure in poly(vinylidene fluoride) (PVDF) in continuous drawing by in situ measurement using synchrotron X-ray radiation with a time resolution of several hundred microseconds. Two neck deformation behaviors were observed in the laser drawing: a moderate neck deformation under low drawing stress and a steep neck deformation under high drawing stress. The low drawing stress resulted in a mixture of α- and β-crystals in which the β-crystal was formed within 1 millisecond after the necking, earlier than the α-crystal. The development of fiber structure under high drawing stress was almost complete in less than 1 millisecond, and the developed structure contained only β-crystals. Small-angle X-ray scattering images showed meridional streaks at low drawing stress, whereas a four-pointed pattern occurred under high drawing stress. Low drawing stress generated a long periodic structure that was defective in the periodic regularity of crystalline and amorphous regions, although the molecular chains were nearly oriented along the fiber axis. The high drawing stress resulted in a well-packed structure of adjacent fibrils with alternating amorphous and crystalline regions.

INTRODUCTION

Poly(vinylidene fluoride) (PVDF) is a noteworthy engineering plastic owing to its excellent properties; namely, good chemical resistance, high mechanical strength and abrasion resistance. In particular, PVDF fiber can be melt-spun to form fishing line because of its low water absorption, low refractive index similar to that of water, high specific gravity, and good resistance to degradation by light. PVDF has been identified to take on five crystalline forms: α, β, γ, δ, and ε [1-4]. The α form (form II) is formed by cooling a quiescent melt, and it forms a nonpolar pseudo-orthorhombic structure containing two chains of tg^+tg^- conformation. Mechanical drawing of the α-form produces the β form (form I) containing two all-*trans* chains. Other forms can be produced by the application of electrical fields [5, 6].

Some studies on the development of structure in PVDF fibers and tapes during melt spinning and deformation have been conducted using simultaneous synchrotron radiation as well as X-ray from laboratory generators for wide-angle X-ray diffraction (WAXD) and small-angle X-ray scattering (SAXS) [7-10]. Cakmak and co-workers [7] have shown that the appearance of the β-phase is stress dependent, first occurring at a spinline stress of 3 MPa and increasing in concentration as stress is increased. The superstructure of the fibers was investigated using small-angle light scattering (SALS), where a transition from a spherulitic structure to a sheaf and rod-like structure was observed with increasing draw ratio. In a later study, Cakmak et al. [8] suggested that PVDF crystallizes with a shish-kebab type morphology, which is a model consisting of a combination of an extended chain crystal (a shish) and folded chain crystals (kebabs) [11], during the melt-spinning process. Schultz and co-workers [10] analyzed the crystal transformation from the α- to the β-form and morphological changes in lamellar and fibrillar structures during deformation at room temperature, and they found that deformation assisted in the conversion from the α- to the β-form. More α- to β-transformation took place in necked regions than in unnecked regions.

Our research group has studied the development of fiber structure in laser-heated drawing for PET running fibers through WAXD and SAXS analyses [12] and afterward for PET and PTT fibers using in situ synchrotron WAXD and SAXS measurement systems [13, 14]. The in situ measurements were conducted as a function of elapsed time calculated from the distance between the measurement and necking positions with high time resolution because the necking could be fixed within a highly confined region by rapid and uniform heating with CO_2 laser radiation (See Figure 3). We succeeded in conducting in situ analyses with time resolutions of 1 ms for X-ray diffraction characterization and 0.47 ms for fiber temperature measurements in PET fibers. This study investigated the development of fiber structure in the vicinity of the necking location for PVDF fiber using our laser drawing system and in situ measurement techniques.

EXPERIMENTAL

Fundamentals of in situ measurement

Figure 1 shows a schematic diagram of the in situ measurement system used in this study. Details of the in situ system can be found in our previous papers [12-14]. The running fiber was heated by irradiation with a CO_2 laser beam generated by a PIN-20S laser source manufactured by Onizca Glass Co. Ltd. The laser source has a rated power of 20±1 W and a laser beam diameter of 5 mm. The running fiber was drawn by speed difference between the feed and take-up rollers. The position of necking induced by laser irradiation was controlled within 1 mm during the drawing. X-ray diffraction images were recorded, and fiber temperature was measured as a function of elapsed time *t*, which was calculated from the

distance D between the necking and measurement positions divided by the fiber running speed v. The distance D varied with necking position, which was changed by moving the laser irradiation.

The time resolution of the continuous drawing was calculated to attain a confidence interval at every measurement point. The time resolution was obtained by dividing the position resolution by take-up speed (m/min). The position resolution W_{x-ray} can be calculated by equation 1 by the width of the X-ray beam W_{beam}, the fluctuation of the necking point W_{neck}, and the length of the necking range W_{deform}.

$$W_{X-ray} = \sqrt{W_{beam}^2 + W_{neck}^2 + W_{deform}^2}$$

eq. 1

In this case, W_{beam} and W_{deform} were 340 and 100 μm, and W_{neck} ranged from 100 to 300 μm. The resulting time resolutions for low and high drawing stress were 0.69 and 0.28 ms, respectively.

Materials and drawing conditions

The PVDF fiber of 250 μm in diameter was kindly provided by Kureha Gohsen Co. Ltd. and drawn to draw ratios of 4.5 and 5.5 with corresponding take-up speeds of 27 and 66 m/min, respectively. Table 1 shows the drawing conditions used in this experiment. Drawing stress was measured by a 3 points type tensiometer (HS-1500S; EIKO SOKKI Co. Ltd.), and the fiber was drawn under two different drawing stresses, that is, high and low drawing stresses of 242 and 110 MPa, respectively. The applied laser intensity was measured with a power meter (PW-250; SYNRAD Co, Ltd.).

Fiber temperature measurement

Fiber temperature was measured using an infrared thermo-spot-sensor (TMZ7-J0-2.5K0.2 type; Japan Sensor Co., Ltd) equipped with an MCT detector and an interference filter. The spot size was 200 μm in diameter, and the response time was 10 ms. The interference filter transmits 3 to 4 μm in wavelength, corresponding to an absorbance band (2500 to 3333 cm^{-1}) representing C-H stretching. The fiber temperature was calculated from the radiation intensity averaged over 30 s for each measurement point. The fiber temperature was calculated in the same way as in the previous study. [11-15]

X-ray diffraction characterization

X-ray diffraction measurements were carried out with synchrotron radiation of BL40B2 in SPring-8. The applied beam was 0.1 nm in wavelength and 340 μm in width. Diffraction images were taken by a 3000×3000 pixel imaging plate attached to a 400 mm long vacuum chamber. The sample-to-detector distance of 419.8 mm was estimated using lead stearate (StPb). The exposure time was 4 min. The neck deformation position was determined by a transmitted X-ray intensity profile through an ion chamber. X-ray images containing diffractions of polyimide film mounted on the vacuum chamber were compensated for by subtracting a blank image.

RESULTS AND DISCUSSION

Neck deformation behavior

Figure 2 shows images from CCD videos taken in the vicinity of the neck deformation. These videos revealed two distinctive appearances depending on drawing stress, with a moderate neck deformation under a low drawing stress of 110 MPa and a steep neck deformation under a high drawing stress of 242 MPa.

CO_2 laser absorption coefficient

The CO_2 laser absorption coefficient for PVDF was characterized using an infrared spectrometer (Shimadzu FT-IR 8400). The CO_2 laser used in this study was 10.6 μm in wavelength, corresponding to 943 cm^{-1}. Infrared absorption spectra were obtained for four PVDF films that were 55, 110, 131, and 198 μm in thickness, and the absorbance at 943 cm^{-1} was extrapolated based on film thicknesses. The results are shown in Figures 3 (a) and (b). The infrared spectra were obtained by ten integrations with a resolution of 2 cm^{-1}. Ultimately, the absorption coefficient for PVDF was found to be 1.908×10^4 m^{-1}.

Fiber temperature profile

Figure 4 shows the fiber temperature profile over time in continuous laser drawing with a high drawing stress at a draw ratio of 5.5, where zero on the horizontal axis indicates the time the necking occurred and the gray-shaded area denotes the region of laser irradiation. The fiber temperature was measured twice to reduce experimental error, and this figure shows these two results together. Before the necking, the fiber temperature increased slightly due to the laser irradiation. At the necking point, that is, at an elapsed time of 0 ms, the fiber temperature showed a sharp rise from about 65 to 85°C, which should result from the plastic deformation of the necking. The fiber temperature continued to increase until 2 ms after necking, when the fiber was leaving the laser irradiation area. The exothermic crystallization seems to have finished at that point. Although the PVDF has a negative T_g of about -35°C, the necking occurred in the range of 65 to 85°C because it is a crystalline polymer. The orientation in the crystalline and amorphous regions increased along the fiber axis with neck deformation. After an elapsed time of around 3 ms the fiber temperature was almost saturated, indicating that the development of the fiber structure was complete.

X-ray diffraction

WAXD analyses

Figures 5 and 6 show X-ray diffraction images of PVDF fibers drawn with low and high drawing stresses, respectively, and their X-ray intensity profiles are shown in Figures 7 and 8, respectively. The X-ray diffraction images revealed a typical PVDF crystal with α-(100)/(020), α-(110), β-(110)/(200), and α-(021) planes. Before the necking, the WAXD images showed an unoriented α-crystal. In Figure 5, the α-(110), β-(110)/(200) diffractions began to concentrate around the equator just after the neck deformation, and the α-(100)/(020) diffraction was concentrated on the equator at 0.5 ms. This result seems to indicate that the diffractions of α-(110), β-(110)/(200), and α-(100)/(020) began to develop immediately after the neck deformation. The α-(021) plane was oriented on the off-meridian after 2.0 ms, which could result from the tg$^+$tg$^-$ conformation of the α-crystal. Figure 7 contains three diffraction peaks along the equatorial direction corresponding to the α-(021), α-(100)/(020), α-(110), and β-(110)/(200) diffractions. The α-(021) diffraction disappeared with neck deformation at the equator. The α-(110) and β-(110)/(200) planes were close to each other and were located in only one peak. Just after the neck deformation, the α-(110), β-(110)/(200) diffraction became

somewhat broad and shifted to a higher 2θ. This shift was caused by the fact that the β-(110)/(200) diffraction intensity increased with elapsed time. Subsequently, the β-crystal was developed immediately after the neck deformation and increased with elapsed time. Ultimately, the β-crystal was dominant in the drawn fiber, although the α- and β- crystals coexisted in the laser-drawn PVDF fiber with the low drawing stress of 110 MPa. Nagaoka and colleagues [17] have reported that the development of crystal structure in laser-drawn PVDF fibers depends on the drawing stress and that drawing stresses higher than 100 MPa largely produce β-crystals. Therefore, the β-crystals developed earlier than the α-crystals in the neck drawing: the β-crystal developed within 1 millisecond after the neck deformation. In Figure 6, the α-(110), β-(110)/(200) diffractions were concentrated on the equator at 0 ms and were well separated from adjacent diffraction, unlike the low drawing stress condition. The diffraction pattern at 0.4 ms clearly revealed the β-crystal formation, and then the pattern hardly changed with elapsed time. Accordingly, the fiber structure development was complete immediately after the neck deformation. The α-crystal diffractions were weak at and after 0.4 ms, and they faded out in the drawn fiber. In Figure 8, we can observe only β-crystals in the drawn fiber.

SAXS analyses

The X-ray diffraction patterns showed some changes in both the SAXS and the WAXD patterns because this characterization used a long distance path of 419 mm. Therefore, we were able to successfully collect SAXS patterns by magnifying the center portion of the X-ray patterns, from which qualitative SAXS analyses can be conducted. Figures 9 and 10 show SAXS images taken in laser drawing with low and high drawing stresses, respectively, and these images show the large-scale periodic character of the structure parallel to the fiber axis. The as-spun fiber showed an appearance of curvature at the meridian, indicating a substantial misorientation of lamella with respect to the fiber axis. In Figure 9, the curvature decreased at 0 and 0.5 ms and then increased and flattened off with elapsed time. Ultimately, the drawn fiber had an appearance of meridional streaks, which may be a precursor of a four-pointed scattering pattern. Thus, the molecular chains were oriented nearly parallel to the fiber axis, and crystalline and amorphous regions alternate in a rather regular manner along the fibril axis. Therefore, in the laser drawing with a low drawing stress of 110 MPa, the long period structure is somewhat defective in the periodic regularity of crystalline and amorphous regions. Adjacent fibrils in the low stress condition seemed not to be as close as those in the high stress condition, and the fibers generated under low stress seemed to be generated after 1 ms.

In Figure 10, on the other hand, the curvature disappeared at the same time as the initiation of neck deformation. SAXS patterns at and after 0 ms presented equatorial streaks, which can be attributed to microvoids generated by drawing under high stress. [10] The streaks decreased with elapsed time, indicating that the microvoids were reduced and concentrated. At and after 0.5 ms, a four-pointed pattern was observed and became increasingly clear with elapsed time. This pattern occurs because adjacent fibrils packed together by alternating amorphous and crystalline regions immediately after the neck deformation, and these regions then became fastened together as time elapsed. In the drawn fiber, the equatorial streak existed clearly even though the four-pointed pattern was completed, and thus, the high drawing stress of 242 MPa may result in a large quantity of microvoids among interlocking fibrils. Furthermore, the high drawing stress may transform the initial lamellar structure into a fibrillar structure after 0.5 ms. This result indicates that the development of the fibrillar structure of PVDF fibers depended on both the drawing stress and the elapsed time.

CONCLUSION

The development of fiber structure in the vicinity of the necking location of PVDF fibers was investigated as a function of elapsed time using the laser drawing system and in situ measurement techniques. Because the necking position was fixed within a highly confined region by rapid and uniform heating with CO_2 laser radiation, we succeeded in conducting in situ analyses with time resolutions of 0.69 and 0.28 ms in the laser-heated drawing of PVDF fibers for drawing stresses of 110 and 242 MPa, respectively. The development of crystal structure observed in WAXD analysis showed that the β-crystal developed immediately after the neck deformation and continued to develop with elapsed time. Ultimately, β-crystals were predominant in the drawn fiber, although the α- and β- crystal forms coexisted in the laser-drawn PVDF fiber produced with a low drawing stress of 110 MPa. For the laser heated neck-drawing of PVDF fibers with a high drawing stress of 242 MPa, the fiber structure development was complete immediately after the neck deformation, and only β-crystals were observed in the drawn fiber. The supramolecular structure elucidated by SAXS indicated that the laser drawing of PVDF fibers with a low drawing stress resulted in a defective long period structure in which adjacent fibrils were farther apart from each other than in the high stress condition. Laser drawing with a high drawing stress produced a four-pointed pattern with an equatorial streak immediately after the neck deformation; that is, the high drawing stress produced a long period structure with a large quantity of microvoids among interlocking fibrils. The fiber structure development in the laser drawing of PVDF fiber depended on the drawing stress and on the elapsed time after necking.

REFERENCES

[1] Lovinger, A. J. Ferroelectric polymers. Science 220, 1115-1121 (1983).

[2] Lovinger, A. J. Crystallization and morphology of melt-solidified poly(vinylidene fluoride). J. Polym. Sci.: Part B: Polym. Phys. 18(4), 793-809 (1980).

[3] Hasegawa, R.; Takahashi, Y.; Chatani, H.; Tadokoro, H. Crystal structure and three crystalline forms of poly(vinylidene fluoride). Polym. J. 3(5), 600-610 (1972).

[4] Weinhold, S.; Litt, M. H.; Lando, J. B. The crystal structure of the γ phase of poly(vinylidene fluoride). Macromolecules 13(5), 1178-1183 (1980).

[5] Doll, W. W.; Lando, J. B. The polymorphism of poly(vinylidene fluoride). II The effect of hydrostatic pressure. J. Macromol. Sci., Phys. 2(2), 219-233 (1968).

[6] Lovinger, A. J. Annealing of poly(vinylidene fluoride) and formation of a fifth phase. Macromolecules 15(1), 40-44 (1982).

[7] Wang, Y.; Cakmak, M.; White, J. M. Structure development in melt spinning poly(vinylidene fluoride) fibers and tapes. J. Appl. Polym. Sci. 30(6), 2615-2632 (1985).

[8] Cakmak, M.; Teitge, A.; Zachmann, H. G.; White J. L. On-line small-angle and wide-angle X-ray scattering studies on melt-spinning poly(vinylidene fluoride) tape using synchrotron radiation. J. Polym. Sci.: Part B: Polym. Phys. 31(3), 371-381 (1993).

[9] Samon, J. M.; Schultz, J. M.; Hsiao, B. S.; Seifert, S.; Stribeck N.; Gurke I.; Collins, G.; Saw C. Structure development during the melt spinning of polyethylene and poly(vinylidene fluoride) fibers by in situ synchrotron small- and wide-angle X-ray scattering techniques. Macromolecules 32(24), 8121-8132 (1999).

[10] Wu, J.; Schultz, J. M.; Yeh, F.; Hsiao, B. S.; Chu, B. In situ simultaneous synchrotron small- and wide-angle X-ray scattering measurement of poly(vinylidene fluoride) fibers under deformation. Macromolecules 33(5), 1765-1777 (2000).

[11] Nagasawa, T.; Shimomura, Y. Mechanism of formation of shish kebab structures. J. Polym. Sci.: Polym Phys. Ed. 12, 2291-2308 (1974).

[12] Yamaguchi, T.; Komoriyama, K.; Ohkoshi, Y.; Urakawa, H.; Gotoh, Y.; Terasawa, N.; Nagura, M.; Kajiwara, K. On-line WAXD / SAXS measurement for CO_2 laser-heated drawing of poly(ethylene terephthalate) fiber. J. Polym. Sci.: Part B: Polym. Phys. 43, 1090-1099 (2005).

[13] Yamaguchi, T.; Kim, K. H.; Murata, T.; Koide, M.; Hitoosa, S.; Urakawa, H.; Ohkoshi, Y.; Gotoh, Y.; Nagura, M.; Kodera, M.; Kajiwara, K. On-line X-ray analysis on the continuous drawing process of poly(ethylene terephthalate) fiber. J. Polym. Sci.: Part B: Polym. Phys. 46, 2126-2142 (2008).

[14] Kim, K. H.; Kang, Y. A.; Murata, T.; Ikehata, S.; Ohkoshi, Y.; Gotoh, Y.; Nagura, M.; Koide, M.; Urakawa, H.; Kodera, M. Initial Structure Development in the CO_2 laser heated drawing of poly(trimethylene terephthalate) fiber. Polymer 49, 5705 (2008),

[15] Okumura, W.; Yamaguchi, T.; Ohkoshi, Y.; Gotoh, Y.; Nagura, M. Direct measurement of fiber temperature in the continuous drawing process of PET fiber heated by CO_2 laser radiation. Int. Polym. Proc. 17(2), 124-132 (2002).

[16] Yamaguchi, T.; Ohkoshi, Y.; Gotoh, Y.; Nagura, M. Online wide-angle X-ray diffraction/small-angle X-ray scattering measurements for the CO_2-laser-heated drawing of poly(ethylene terephthalate) fiber. Seikei-Kakou. 17, 649-653 (2005).

[17] Nagaoka, A.; Konuma, H.; Ikaga, T.; Nakata, K.; Ohkoshi, Y.; Gotoh, Y.; Nagura, M.; Masumura, N.; Kokuno, Y.; Structure and solid-state properties of poly(vinylidene fluoride) fiber drawn with CO_2 laser heating. Seikeikakou Symposia, 307-308 (2005).

FIGURE LEGENDS

Figure 1. Schematic diagram of the on-line measurement system. The elapsed time after the neck deformation can be calculated from the distance D between the neck deformation location and the measuring positions divided by the fiber running speed v.

Figure 2. CCD video images in the vicinity of neck deformation with low (a) and high (b) drawing stresses.

Figure 3. Infrared absorption spectra (a) and absorbance at 943 cm^{-1} (b) as a function of film thickness. Film thicknesses are noted on the right side of individual spectra.

Figure 4. Fiber temperature profile as a function of elapsed time, where zero on the horizontal axis indicates neck deformation and the gray-shaded area denotes the laser-irradiated region.

Figure 5. X-ray diffraction images taken at various elapsed times during continuous laser drawing under low drawing stress.

Figure 6. X-ray diffraction images taken at various elapsed times during continuous laser drawing under high drawing stress.

Figure 7. X-ray intensity profiles along the equatorial (a) and meridional (b) directions for low drawing stress.

Figure 8. X-ray intensity profiles along the equatorial (a) and meridional (b) directions for high drawing stress.

Figure 9. SAXS patterns for low drawing stress (magnified images of Figure 6).
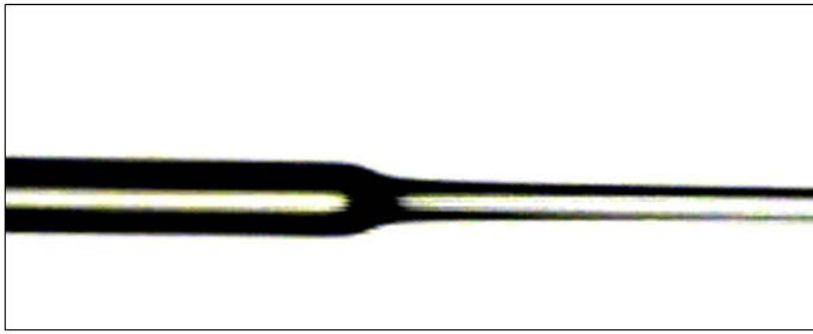
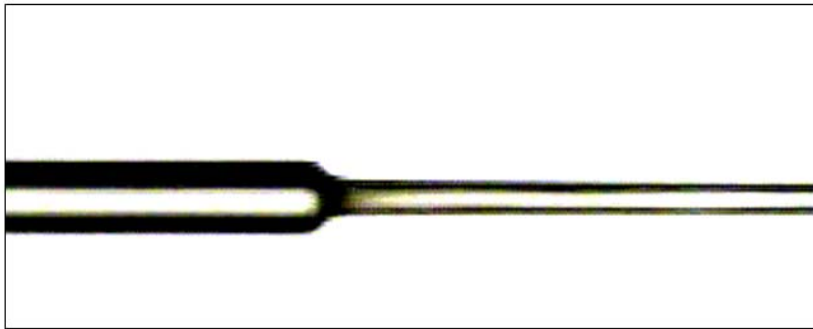**Figure 10.** SAXS patterns for high drawing stress (magnified images of Figure 7).

TABLE LEGEND

Table 1. Drawing conditions for the laser drawing of PVDF fibers.
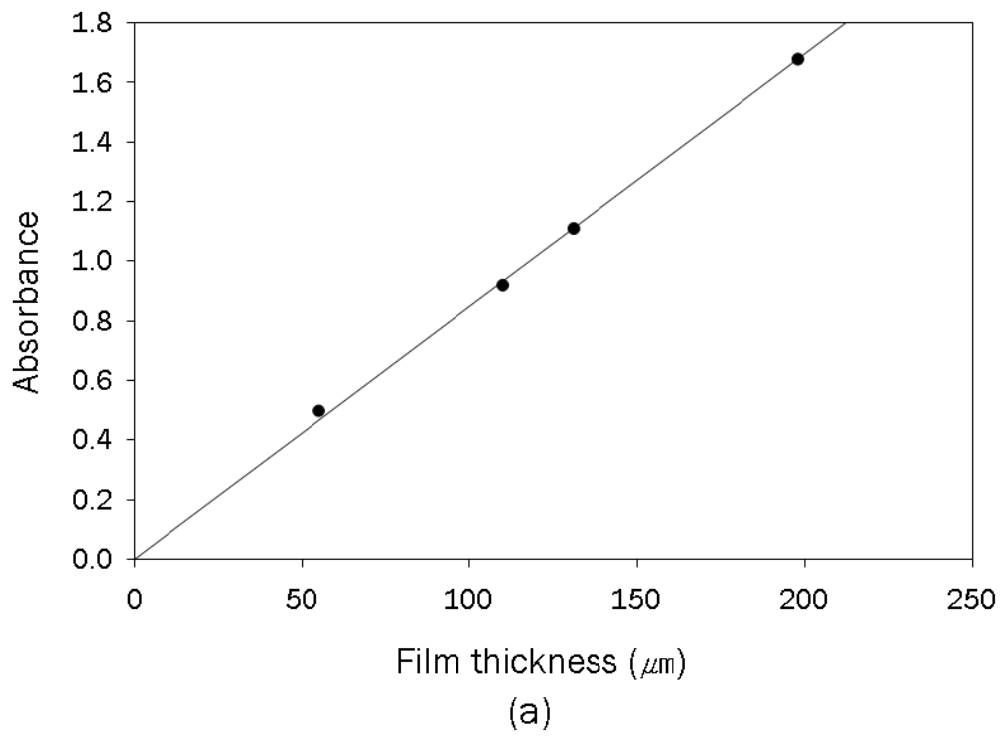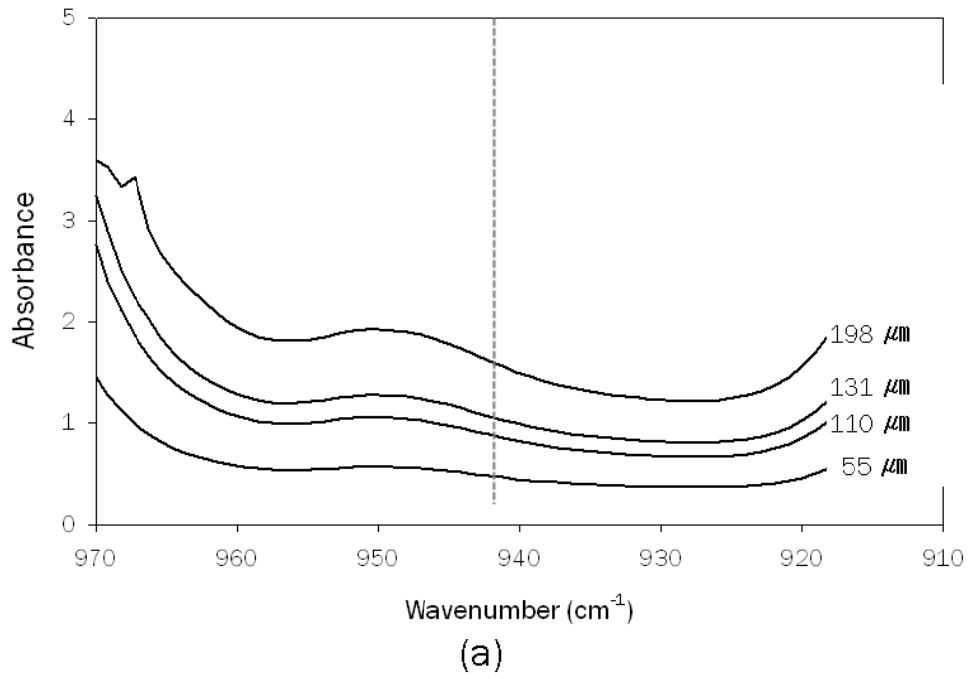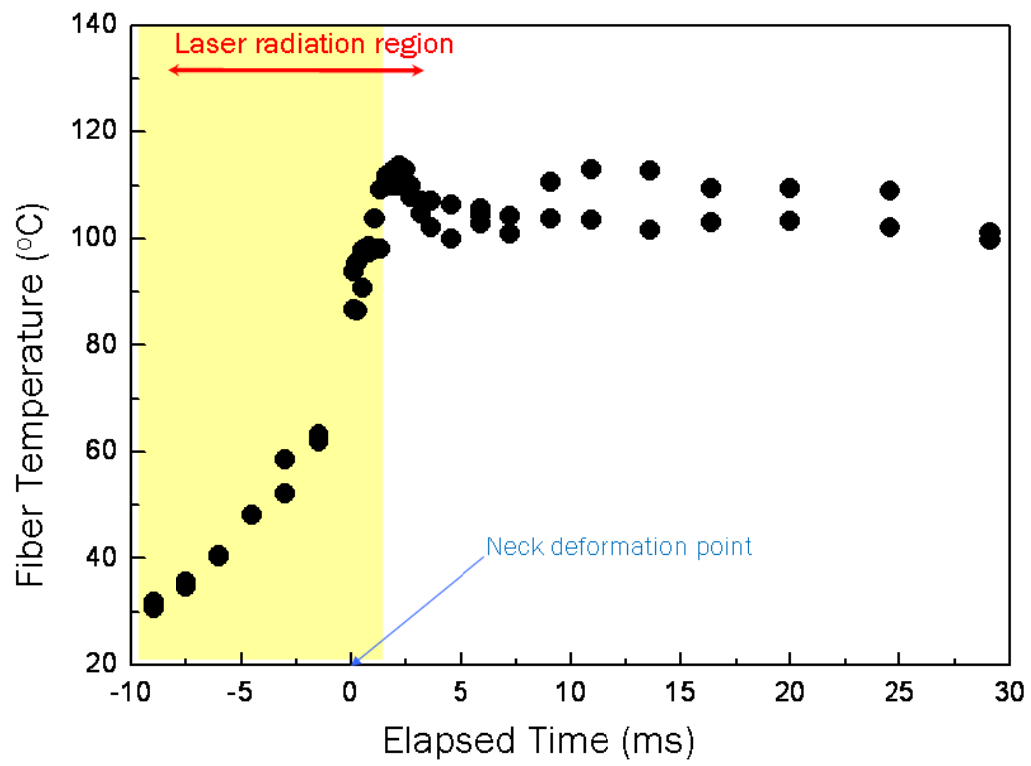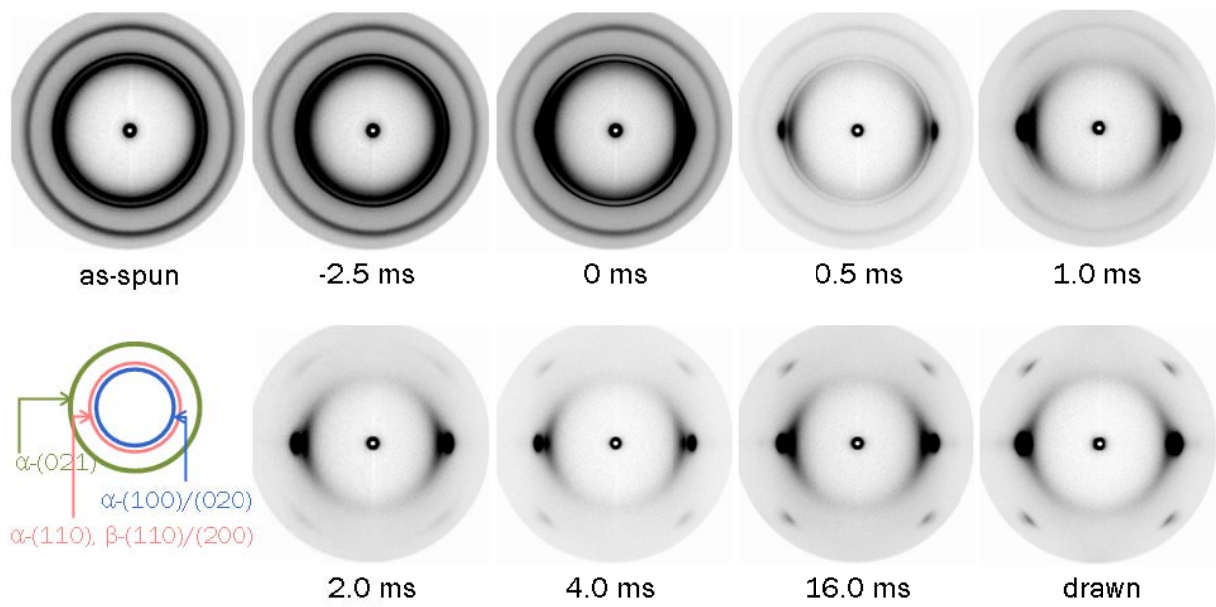
Figure 1.

(a)

(b)

Figure 2.

(a)

Film thickness (μm)

(a)

Figure 3.

Figure 4.

as-spun   -2.5 ms   0 ms   0.5 ms   1.0 ms

α-(021)
α-(100)/(020)
α-(110), β-(110)/(200)

2.0 ms   4.0 ms   16.0 ms   drawn

Figure 5.

as-spun   -2.5 ms   0 ms   0.5 ms   1.0 ms

α-(021)

α-(100)/(020)

α-(110), β-(110)/(200)

2.0 ms   4.0 ms   16.0 ms   drawn
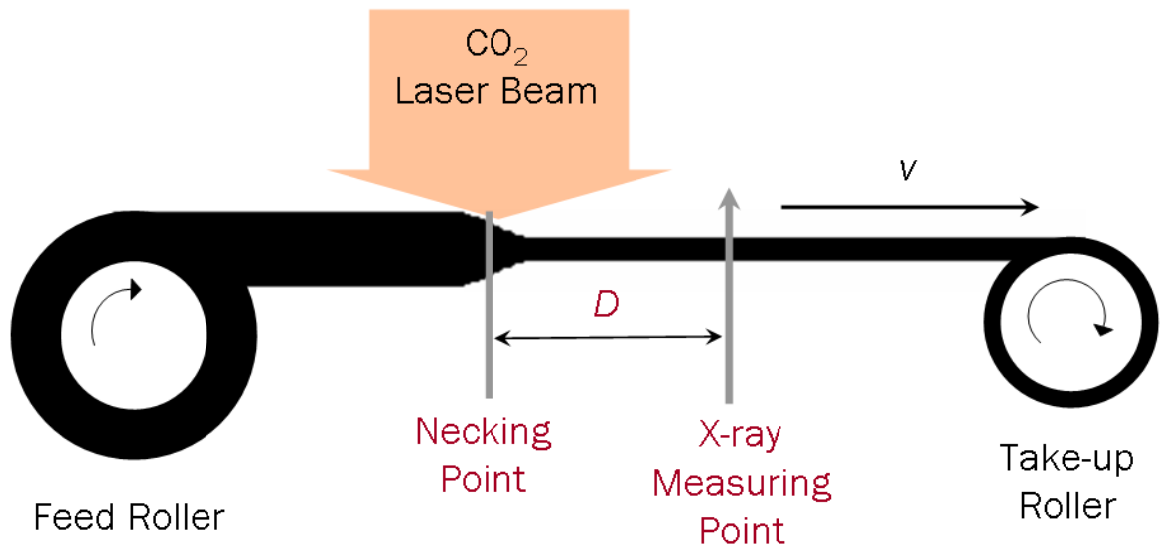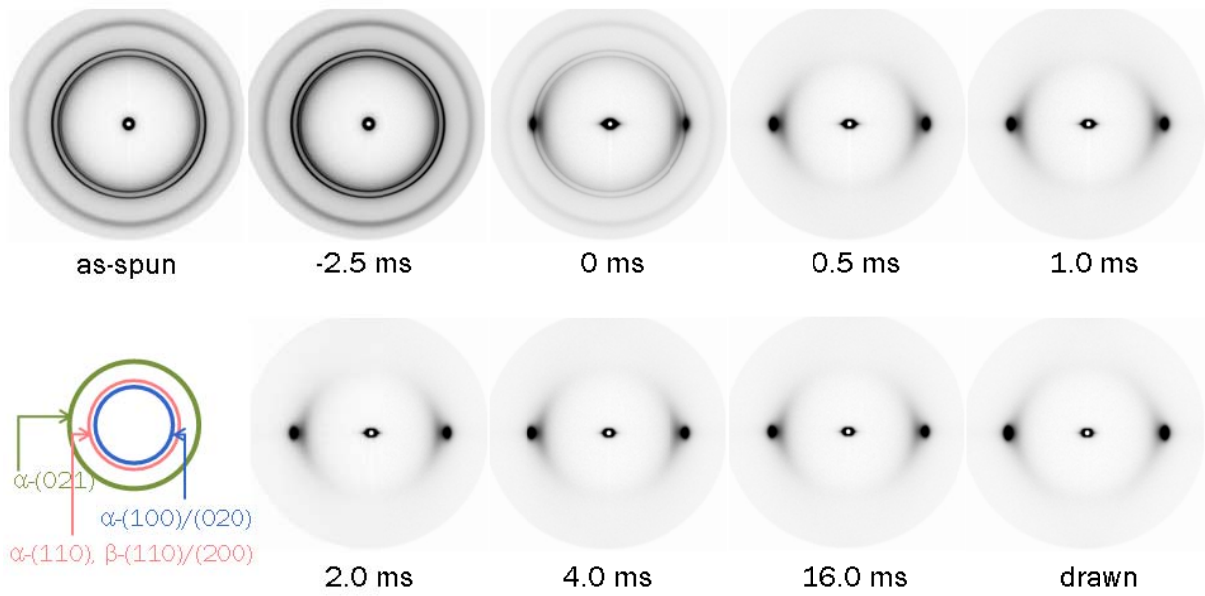
Figure 6.

Figure 7.

Figure 8.

as-spun   -2.5 ms   0 ms   0.5 ms   1.0 ms

2.0 ms   4.0 ms   16.0 ms   drawn

Figure 9.

| as-spun | -2.5 ms | 0 ms | 0.5 ms | 1.0 ms |

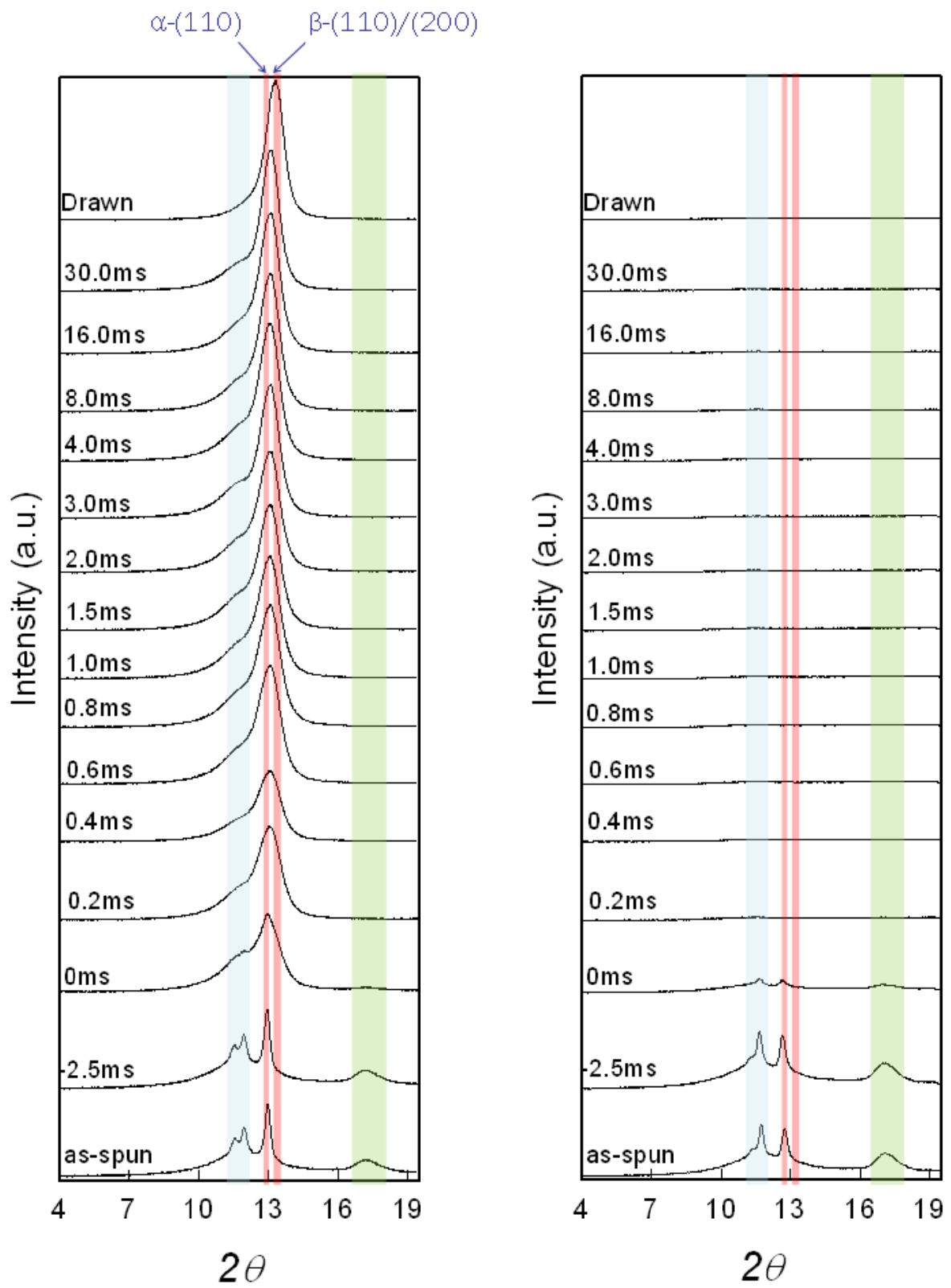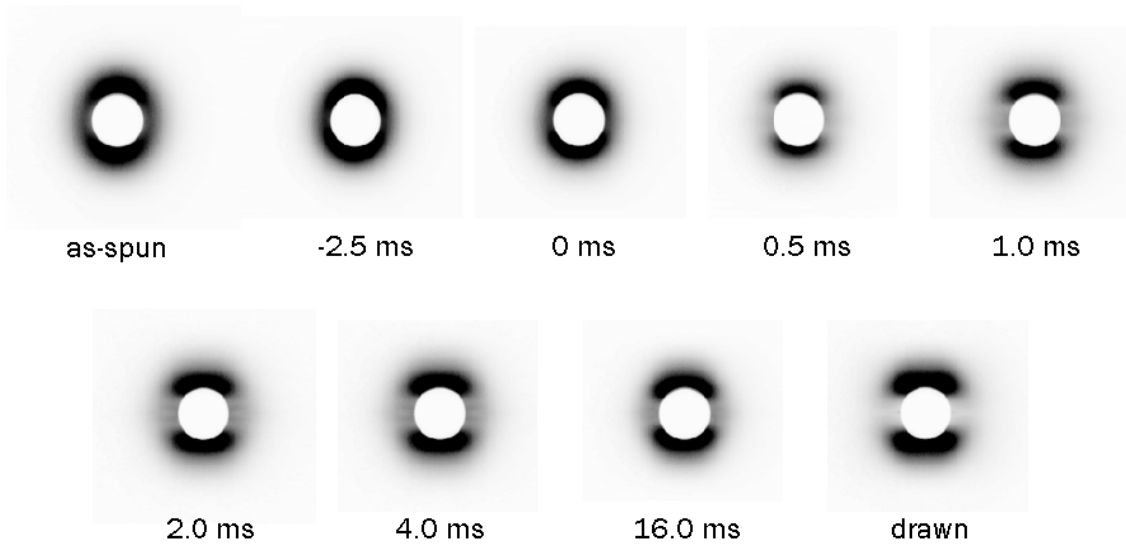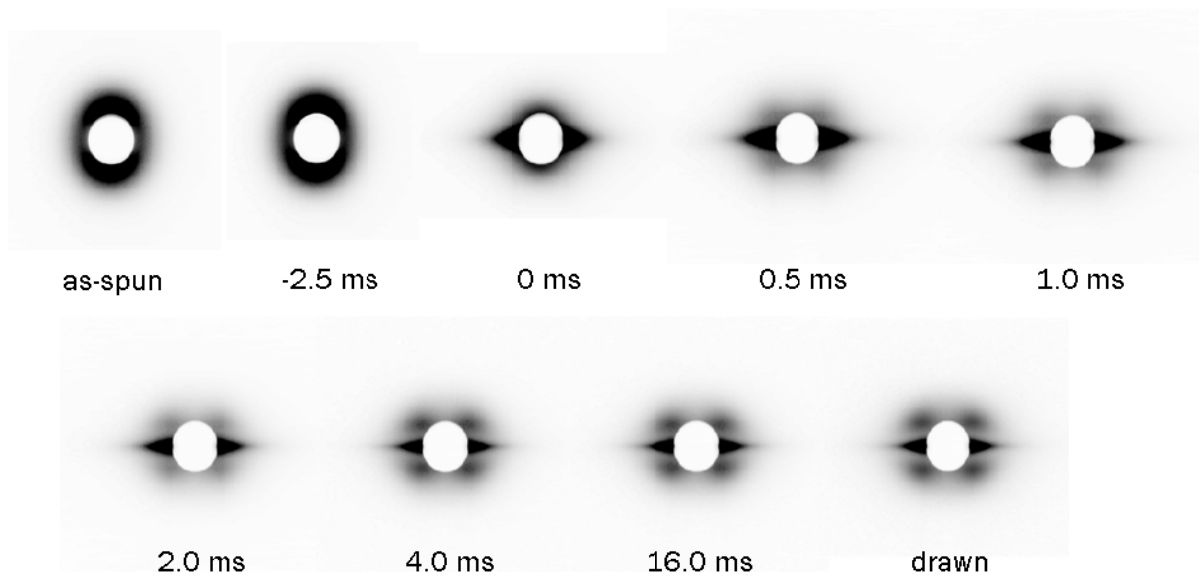| 2.0 ms | 4.0 ms | 16.0 ms | drawn |
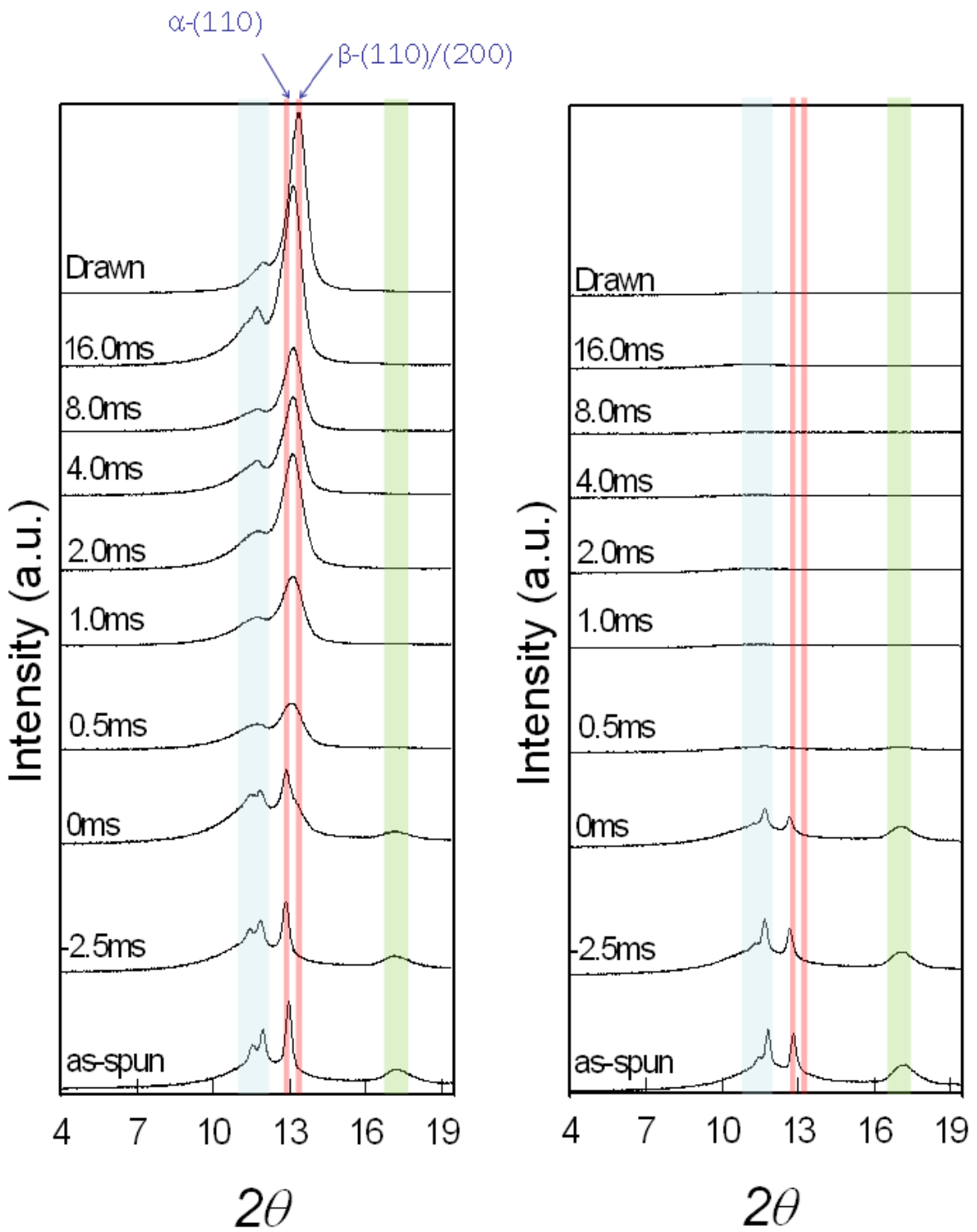
Figure 10.

Table 1.

Drawing stress (MPa)	Draw ratio	Feed speed (m/min)	Take-up speed (m/min)	Time accuracy (ms)
110	4.5	6	27	0.69
242	5.5	12	66	0.28